DNA damage in stem cells activates p21, inhibits p53, and induces symmetric self-renewing divisions

Alessandra Insinga[a,1], Angelo Cicalese[a,1], Mario Faretta[a], Barbara Gallo[a], Luisa Albano[a], Simona Ronzoni[a], Laura Furia[a], Andrea Viale[a,2], and Pier Giuseppe Pelicci[a,b,3]

[a]Department of Experimental Oncology, European Institute of Oncology, 20141 Milan, Italy and [b]Dipartimento di Medicina, Chirurgia, e Odontoiatria, Università degli Studi di Milano, 20122 Milan, Italy

Edited* by Carlo M. Croce, The Ohio State University, Columbus, OH, and approved January 17, 2013 (received for review August 7, 2012)

DNA damage leads to a halt in proliferation owing to apoptosis or senescence, which prevents transmission of DNA alterations. This cellular response depends on the tumor suppressor p53 and functions as a powerful barrier to tumor development. Adult stem cells are resistant to DNA damage-induced apoptosis or senescence, however, and how they execute this response and suppress tumorigenesis is unknown. We show that irradiation of hematopoietic and mammary stem cells up-regulates the cell cycle inhibitor p21, a known target of p53, which prevents p53 activation and inhibits p53 basal activity, impeding apoptosis and leading to cell cycle entry and symmetric self-renewing divisions. p21 also activates DNA repair, limiting DNA damage accumulation and self-renewal exhaustion. Stem cells with moderate DNA damage and diminished self-renewal persist after irradiation, however. These findings suggest that stem cells have evolved a unique, p21-dependent response to DNA damage that leads to their immediate expansion and limits their long-term survival.

Adult stem cells (SCs) are thought to be resistant to DNA damage (DD)-induced apoptosis or senescence owing to the activation of unique pro-survival and DD repair (DDR) responses (1–3). Genetic alterations that decrease DNA repair activities lead to increased DD and reduced self-renewal in SCs, suggesting that DDR is critical to preservation of SC function (1, 4, 5). DDR decreases during physiological aging, a phenomenon correlated with the accumulation of endogenous DD and decreased self-renewal in aged SCs (6–9).

In differentiated cells, DD triggers a checkpoint response that leads to apoptosis or senescence and depends on activation of the tumor suppressor p53 (10). This is considered a powerful tumor-suppressor mechanism, as demonstrated by the finding that p53 is invariably inactivated in spontaneous tumors (11). After irradiation, p53 is up-regulated in populations enriched for hematopoietic, hair follicle bulge, and colon SCs (5, 12–15). Whether this is critical for activation of the DDR response and maintenance of self-renewal, why p53 induction does not result in SC apoptosis or senescence, and how tumor suppression is executed in SCs remain unclear, however. Indirect evidence indicates that the cell cycle inhibitor p21, a downstream effector of p53, might be involved in DD processing in SCs. In the absence of p21, SCs exhaust prematurely (16) and after a low radiation dose display reduced reconstitution capacity (17). Here we report our studies on the role of p53 and p21 in DD processing of highly purified hematopoietic SCs (HSCs) and mammary SCs (MaSCs).

Results

X-Rays Induce p53-Independent Up-Regulation of p21 in HSCs. To investigate p21 and p53 regulation in HSCs after DD, we treated mice with X-rays using the maximal sublethal dose of 5.5 Gy (*SI Appendix*, Fig. S1). After 6 h, mice were killed, and bone marrow (BM) mononuclear cells (MNCs) were FACS-sorted to obtain highly purified populations of HSCs [long-term reconstituting HSCs (LT-HSCs), Lin^-/c-Kit^+/$Sca\text{-}1^+$/$Flk2^-$/$CD34^-$ and short-term reconstituting HSCs (ST-HSCs), Lin^-/c-Kit^+/$Sca\text{-}1^+$/$Flk2^-$/$CD34^+$] and progenitors [multipotent progenitors (MPPs), Lin^-/c-Kit^+/$Sca\text{-}1^+$/$Flk2^+$/$CD34^+$ and common myeloid progenitors (CMPs), Lin^-/c-Kit^+/$Sca\text{-}1^-$). In a parallel approach (ex vivo), MNCs were extracted immediately after X-ray treatment, incubated for 6 h in vitro, and then processed. Expression and intracellular localization of relevant proteins were analyzed by conventional immunofluorescence (IF) and, in selected experiments, image cytometry, a recently developed protocol that allows automated acquisition and analysis of thousands of cell images (*SI Appendix*, *SI Materials and Methods*).

We first investigated levels of activated p53, using antibodies against phosphorylated p53 (P-p53). As expected, progenitors had up-regulated P-p53 at 6 h after irradiation (in vivo, ∼60% of MPPs and ∼70% of CMPs; ex vivo, ∼80% and ∼70%, respectively) (Fig. 1*A*). Unexpectedly, p53 was not activated in the LT-HSCs at the same time point, with only ∼10% P-p53–positive cells (Fig. 1*A*). Notably, the intensity of the P-p53 signal was approximately twofold to threefold lower in these rare positive cells than in irradiated progenitors (Fig. 1*B* and *SI Appendix*, Fig. S2). p53 levels were confirmed by Western blot analysis (Fig. 1*C*).

Considering that this diversity between HSCs and progenitors could reflect different kinetics of p53 activation, we analyzed the time courses of p53 activation on X-rays. LT-HSCs did not activate p53 within 12 h of cessation of irradiation. In contrast, progenitors showed a sharp peak of p53 activation between 3 and 6 h that disappeared after 6 h (Fig. 1*A*).

Predictably, X-rays also induced substantial activation of p21 in the progenitors, both in vivo and ex vivo, as shown by IF (∼60–70% of MPPs and CMPs at 6 h) (Fig. 1*A*) and quantitative PCR (qPCR) (Fig. 1*D*), with kinetics comparable to that of p53 activation (Fig. 1*A*). Strikingly, however, despite no p53 activation, p21 was strongly activated in irradiated LT-HSCs as well (∼50% in vivo and ∼70% ex vivo) and was long-lasting; ∼60% of LT-HSCs remained p21-positive between 3 and 12 h postirradiation (Fig. 1*A*). Analysis of the role of p53 in X-ray–induced p21 up-regulation using $p53^{-/-}$ mice showed that p21 activation was p53-dependent in progenitors but p53-independent in LT-HSCs (Fig. 1 *D* and *E* and *SI Appendix*, Fig. S3*A*). Taken together, these data (i.e, absence of p53 activation and p53-independent p21 up-regulation) demonstrate the existence of p53 and p21 regulatory systems specific to LT-HSCs, which, being conserved in the ex vivo experimental setting as well, reflect cell-autonomous mechanisms.

p21 Up-Regulation in HSCs Inhibits X-Ray–Induced p53 Activation and Prevents Apoptosis. We next investigated the effect of X-rays on apoptosis, by immunostaining for cleaved caspase-3 (C3).

Author contributions: A.I., A.C., M.F., A.V., and P.G.P. designed research; A.I., A.C., M.F., B.G., L.A., S.R., L.F., and A.V. performed research; M.F. and L.F. contributed new reagents/analytic tools; A.I., A.C., M.F., B.G., L.A., S.R., A.V., and P.G.P. analyzed data; and A.I., A.C., and P.G.P. wrote the paper.

The authors declare no conflict of interest.

*This Direct Submission article had a prearranged editor.

[1]A.I. and A.C. contributed equally to this work.

[2]Present address: Department of Genomic Medicine, The University of Texas M.D. Anderson Cancer Center, Houston, TX 77030.

[3]To whom correspondence should be addressed. E-mail: piergiuseppe.pelicci@ieo.eu.

This article contains supporting information online at www.pnas.org/lookup/suppl/doi:10.1073/pnas.1213394110/-/DCSupplemental.

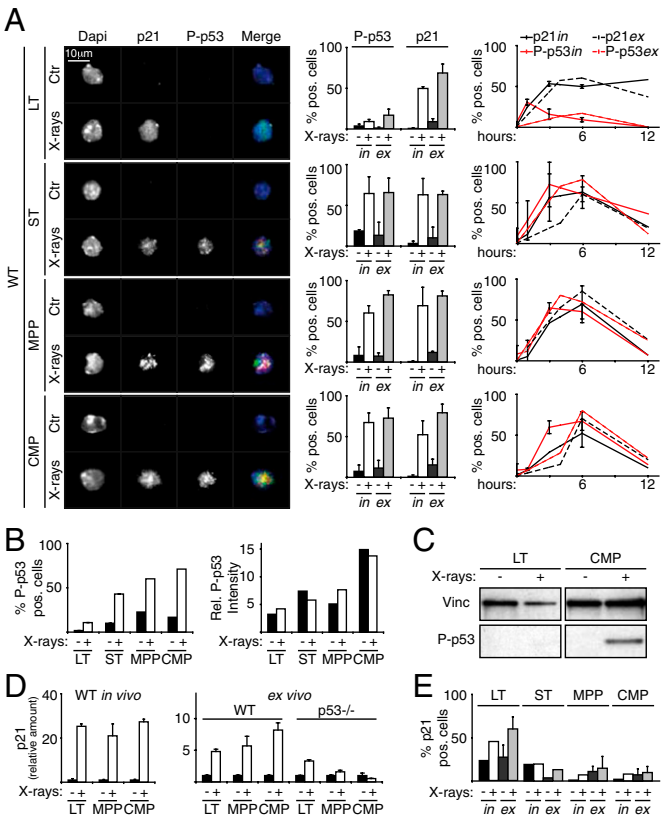

Fig. 1. X-rays induce P-p53–independent up-regulation of p21 in HSCs. (*A*) (*Left*) IF of P-p53 or p21 expression in control (Ctr) and irradiated (at 6 h) WT LT-HSCs, ST-HSCs, MPPs, and CMPs (in vivo experiment; green, α-p21; red, α-Pp53; blue, DAPI; original magnification 100×). (*Center*) Percentages of p53- and p21-positive cells from both in vivo (*in*) and ex vivo (*ex*) experiments. (*Right*) Time course of p53 and p21 activation in the same cell types from in vivo (*in*) and ex vivo (*ex*) experiments. (*B*) Image cytometry quantification of frequency and intensity of P-p53–positive cells in Ctr and irradiated LT-HSCs, ST-HSCs, MPPs, and CMPs (*SI Appendix*, Fig. S2); in vivo experiment. Note that the intensity of P-p53 staining in the rare positive cells before irradiation is comparable to that observed after irradiation in all subpopulations. (*C*) Western blot analysis of P-p53 in LT-HSCs and CMPs at 6 h after in vivo irradiation. Vinc, vinculin. (*D*) qPCR analysis of p21 induction in WT and $p53^{-/-}$ LT-HSCs, MPPs, and CMPs at 6 h after irradiation. p21 transcription was analyzed both in vivo (*Left*) and ex vivo (*Right*). (*E*) Percentage of p21-positive cells in Ctr and irradiated $p53^{-/-}$ LT-HSCs, ST-HSCs, MPPs, and CMPs. Experimental conditions were the same as in *A*. In *A*, *D*, and *E*, data are expressed as mean ± SD of biological triplicates. The in vivo (*in*) and ST-HSC ex vivo (*ex*) data shown in E are representative of three independent experiments; data in B are representative of two independent experiments.

We observed massive apoptosis of MPPs and CMPs at 6 h after X-ray exposure in both in vivo and ex vivo experiments (Fig. 2*A*). Apoptosis was p53-dependent, being abrogated in progenitors from irradiated $p53^{-/-}$ mice. In contrast, LT-HSCs from WT and $p53^{-/-}$ mice were resistant to X-ray–induced apoptosis (Fig. 2*A*), and this effect was not transient (Fig. 2*B*). Finally, we investigated whether LT-HSC radioresistance was related to lower levels of DD in these cells or to their quiescence (18). Image cytometry analysis of γH2AX, a surrogate marker of double-strand breaks, showed no significant differences between LT-HSCs and MPPs in terms of percentage of positive cells or signal intensity (Fig. 2*C*). In vivo administration of the cytokine G-CSF induced proliferation of LT-HSCs (~10–60% cells positive for the proliferation marker Ki67) in the absence of detectable effects on DD, which remained mostly resistant to X-ray–induced apoptosis (Fig. 2*D*). Thus, our data do not support either hypothesis (low DD or quiescence), but rather corroborate the conclusion that LT-HSCs are resistant to X-ray–induced apoptosis. Consistently, proapoptotic p53 target genes (i.e., *Noxa*, *Puma*, *Bax*, and *Bim*) were not activated in these cells (*SI Appendix*, Fig. S4).

We next examined the role of p21 in LT-HSC radioresistance. Strikingly, at 6 h after in vivo irradiation, $p21^{-/-}$ LT-HSCs showed considerable up-regulation of P-p53 (~60%); robust induction of the proapoptotic *Noxa*, *Puma*, *Bax*, and *Bim* genes; inhibition of the antiapoptotic *Bcl-xL* gene; and massive (~60%) apoptosis (Fig. 2*E* and *SI Appendix*, Fig. S3*B* and S4). Accordingly, $p21^{-/-}$ mice did not survive the 5.5-Gy irradiation (*SI Appendix*, Fig. S1). Taken together, these results demonstrate that after irradiation, a specific p21-dependent response is initiated in LT-HSCs that prevents activation of p53 and apoptosis.

Purified ST-HSCs exhibited both activation of p53 and p53-dependent up-regulation of p21 (Fig. 1 *A*, *B*, and *E*), as was seen in MPPs and CMPs. Strikingly, however, despite p53 induction, ST-HSCs were radioresistant, with their radioresistance dependent on p21 expression, as in LT-HSCs (Fig. 2*A*). The mechanisms underlying DD responses in ST-HSCs were not investigated further in this study.

Similar Regulation of p53, p21, and Apoptosis in MaSCs as in HSCs After X-Ray Exposure. MaSCs from primary mammary tissues can be propagated in nonadherent culture conditions and are the sole cells that survive after seeding. They maintain self-renewing capacities and expand clonally to form mammospheres consisting of MaSCs and differentiated progeny or progenitors (~1 MaSC and ~300 progenitor cells per spheroid). Homogenous populations of MaSCs can be obtained from mammospheres using established label-retaining protocols (PKH assay) (19).

WT primary mammospheres (M1) labeled with the red fluorescent dye PKH-26 (PKH) were disaggregated, irradiated, and after 6 h sorted into PKH^{high} (corresponding to MaSCs) and PKH^{low} (corresponding to progenitors) populations. IF showed activation of p21 after X-ray exposure in ~60% of both MaSCs and progenitor cells (Fig. 3*A*) and activation of p53 in progenitor cells, but not in MaSCs (Fig. 3*B*). Accordingly, analysis of $p53^{-/-}$ MaSCs confirmed that p21 induction was p53-independent (Fig. 3*A*).

Anti-C3 immunostaining showed resistance of PKH^{high} cells to X-ray–induced apoptosis, with ~5% C3-positive cells in PKH^{high} cells, compared with ~50% in PKH^{low} cells (Fig. 3*C*). Accordingly, X-rays did not affect the numbers of secondary mammospheres (M2) obtained after replating (Fig. 3*D* and *SI Appendix*, Fig. S5). Importantly, similar to the LT-HSCs, analysis of $p53^{-/-}$ and $p21^{-/-}$ mammospheres showed that p53 activation was suppressed by p21 in PKH^{high} cells (Fig. 3*B*), and that radioresistance was p21-dependent and p53-independent (Fig. 3*D*). Of note, the radioresistance of WT MaSCs was abrogated by silencing of p21 expression, whereas the radiosensitivity of $p21^{-/-}$ MaSCs was rescued by reexpression of WT p21 (*SI Appendix*, Fig. S6). These findings indicate that both HSCs and MaSCs have a unique, p21-dependent DD response that inhibits p53 activation and prevents cell depletion.

p21 Up-Regulation in HSCs Limits DD and Maintains Self-Renewal After Irradiation. We next studied the role of p21 and p53 in HSC DDR and self-renewal. DDR was assessed indirectly by measuring persistent DD in LT-HSCs at 2 mo after irradiation with 4.5 Gy, the maximal sublethal dose for our $p21^{-/-}$ mice (*SI Appendix*, Fig. S1). At 6 h after irradiation, LT-HSCs were ~100% γH2AX-positive (more than four foci per cell) in all strains (Fig. 4*A*). By 2 mo later, these positive cells had almost disappeared among WT and $p53^{-/-}$ LT-HSCs (~4% and ~8%, respectively), but remained detectable in ~40% of $p21^{-/-}$ LT-HSCs (Fig. 4*A*). This indicates that DDR is impaired in irradiated $p21^{-/-}$, but not $p53^{-/-}$, LT-HSCs. γH2AX-positive progenitors of all strains virtually disappeared after 2 mo (*SI Appendix*, Fig. S7 *A* and *B*).

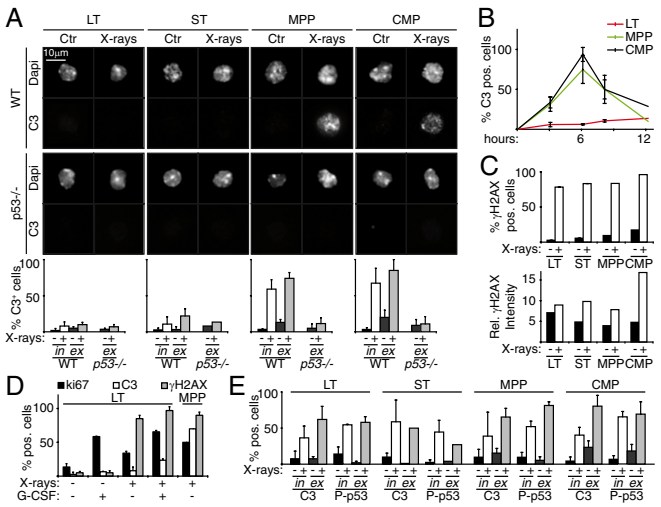

Fig. 2. p21 up-regulation in HSCs inhibits X-ray–induced p53 activation and prevents apoptosis. (*A*) Images: IF of cleaved C3 in Ctr and irradiated (at 6 h) WT and p53 $^{-/-}$ LT-HSCs, ST-HSCs, MPPs, and CMPs; in vivo experiment. Graphs: Percentage of C3-positive cells from both in vivo (*in*) and ex vivo (*ex*) experiments. (*B*) Time course of C3 activation in WT LT-HSCs, ST-HSCs, MPPs, and CMPs, analyzed by IF (ex vivo experiment). (*C*) Image cytometry quantification of frequency (*Upper*) and intensity (*Lower*) of γH2AX-positive cells in Ctr and irradiated LT-HSCs, ST-HSCs, MPPs, and CMPs. Note that the intensity of γH2AX staining in the rare positive cells before irradiation is in the range of that observed after irradiation in all subpopulations, suggesting a similar extent of spontaneous DD and X-ray–induced DD. (*D*) IF of Ki67, C3, and γH2AX expression in Ctr and irradiated LT-HSCs from mice treated and not treated with G-CSF (expressed as percentage of positive cells). MPPs from irradiated mice served as internal controls. (*E*) IF of C3 and P-p53 in ctr and irradiated (at 6 h) p21$^{-/-}$ LT-HSCs, ST-HSCs, MPPs, and CMPs from both in vivo (*in*) and ex vivo (*ex*) experiments, expressed as percentage of positive cells. Data in *A*, *B*, *D*, and *E* are expressed as mean ± SD of biological triplicates; data in *C* are representative of two independent experiments.

We analyzed HSC function at the same time point (2 mo after irradiation) by competitive repopulation assays. For this, donor cells (nonirradiated or irradiated WT or p21$^{-/-}$ MNCs in a Ly5.2 background) were cotransplanted with WT competitor MNCs (Ly5.1) into irradiated recipients. Engraftment was assessed 4 mo later by analysis of the Ly5.1/2 chimerism in the peripheral blood. Nonirradiated WT or p21$^{-/-}$ samples demonstrated equal repopulation abilities [repopulating units (RU), ∼30] (Fig. 4*B*). In contrast, the repopulation ability of irradiated p21$^{-/-}$ samples was significantly reduced compared with the irradiated WT samples (RU, ∼4 vs. ∼10) (Fig. 4*B*). Similar results were observed after direct comparison of irradiated p21$^{-/-}$ MNCs with irradiated WT MNCs using irradiated WT MNCs as a competitor (RU_{WT}, ∼10; $RU_{p21^{-/-}}$, ∼4) (Fig. 4*B*).

To test whether the diminished repopulating capacities of p21$^{-/-}$ MNCs are related to reduced HSC self-renewal, we analyzed these cells' ability to form phenocopies of themselves in primary transplant recipients. We transplanted MNCs from irradiated WT and p21$^{-/-}$ mice into irradiated WT mice. At 4 mo after transplantation, the number of donor p21$^{-/-}$ LT-HSCs was approximately fourfold lower than that of donor WT LT-HSCs (Fig. 4*B*). Thus, as observed for DDR activities, self-renewal was impaired in irradiated p21$^{-/-}$ LT-HSCs.

The competitive repopulation assay also showed a significant drop in the repopulation ability of the WT BM after irradiation, from ∼30 to RU ∼10 RU (Fig. 4*B*), as expected (3). To investigate whether this drop is correlated with DD persistence in WT LT-HSCs, as observed in the p21$^{-/-}$ LT-HSCs (Fig. 4*A*), we reevaluated DD in LT-HSCs using a lower detection threshold (two or more γH2AX foci per cell). Our results indicated persistence of DD in both WT LT-HSCs (∼32%) and p21$^{-/-}$ LT-HSCs (∼67%) (Fig. 4*C*). Thus, DDR is not flawless in irradiated WT LT-HSCs, and appears to be further impaired in irradiated p21$^{-/-}$ LT-HSCs. Of note, under steady-state conditions (e.g., before irradiation), the frequency of DD-positive LT-HSCs was significantly higher in the p21$^{-/-}$ BM compared with WT (∼38% vs. ∼14%; $P < 0.05$) (Fig. 4*C*), suggesting that p21 is also involved in the processing of DD generated by endogenous cellular activities. Accordingly, DD accumulation in LT-HSCs during physiological aging (2, 4, and 24 mo) was significantly more evident in p21$^{-/-}$ mice (Fig. 4*C*).

These results suggest that p21 regulates the cellular response to DD in LT-HSCs, limiting DD accumulation and preventing exhaustion of their self-renewal competence. At the end of this response, however, HSCs display moderate levels of DD and reduced self-renewal, suggesting that the lifespan of SCs is limited by the suboptimal DD response.

Similar Effects of p21 on DD Accumulation and Self-Renewal in MaSCs. We analyzed the effects of X-rays on DD and self-renewal in MaSCs. Primary mammary epithelial cells were PKH-labeled and plated to form M1, and irradiated and replated to form M2. At 6 h after irradiation, accumulation of γH2AX foci (more than four foci per cell) was seen in nearly all PKH^{high} and PKH^{low} cells from both WT and p21$^{-/-}$ samples (Fig. 4*D* and *SI Appendix*, Fig. S7*C*). However, at the end of the week in culture, γH2AX foci were almost completely absent in WT PKH^{high} and PKH^{low} cells but remained detectable in ∼60% of the PKH^{high} and PKH^{low} cells from the p21$^{-/-}$ M2 samples (Fig. 4*D* and *SI Appendix*, Fig. S7*C*). By also including less-damaged cells (two or more H2AX foci per cell), the frequency of cells with persistent DD reached ∼20% in the WT PKH^{high} cells, compared with ∼70% in the p21$^{-/-}$ PKH^{high} cells (*SI Appendix*, Fig. S7*D*). Accordingly, serial replating of irradiated M1 showed a significant reduction in the efficiency of mammosphere formation in WT MaSCs (detected

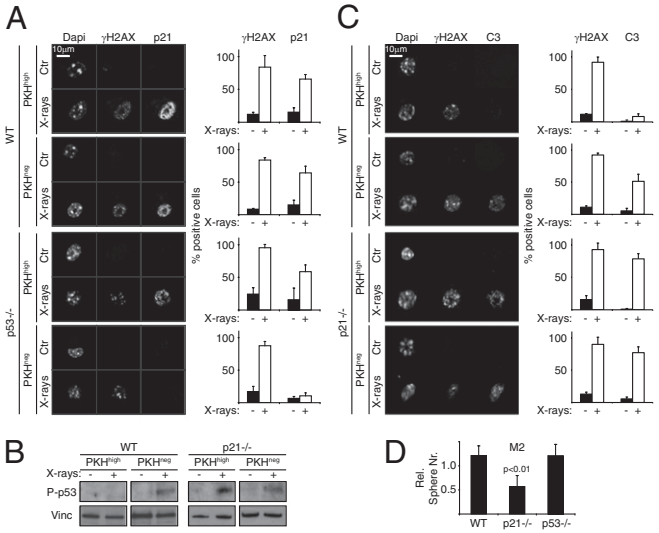

Fig. 3. Regulation of p53, p21, and apoptosis is similar in MaSCs and HSCs after irradiation. (*A*) (*Left*) IF of γH2AX and p21 expression in Ctr and irradiated (4 Gy, at 6 h) WT and p53$^{-/-}$ MaSCs (PKH^{high}) and progenitors (PKH^{low}). (*Right*) Percentage of positive cells. (*B*) Western blot analysis of P-p53 in WT and p21$^{-/-}$ MaSCs (PKH^{high}) and progenitors (PKH^{low}) at 6 h after irradiation. Vinc, vinculin. (*C*) (*Left*) IF of γH2AX and C3 expression in Ctr and irradiated (4 Gy, at 6 h) WT and p21$^{-/-}$ MaSCs (PKH^{high}) and progenitors (PKH^{low}). (*Right*) Percentage of positive cells. (*D*) Relative numbers of M2 obtained from irradiated (4 Gy) WT, p21$^{-/-}$, and p53$^{-/-}$ M1, normalized to untreated samples. Data are expressed as mean ± SD of three independent experiments. *P* values were calculated using the Student *t* test.

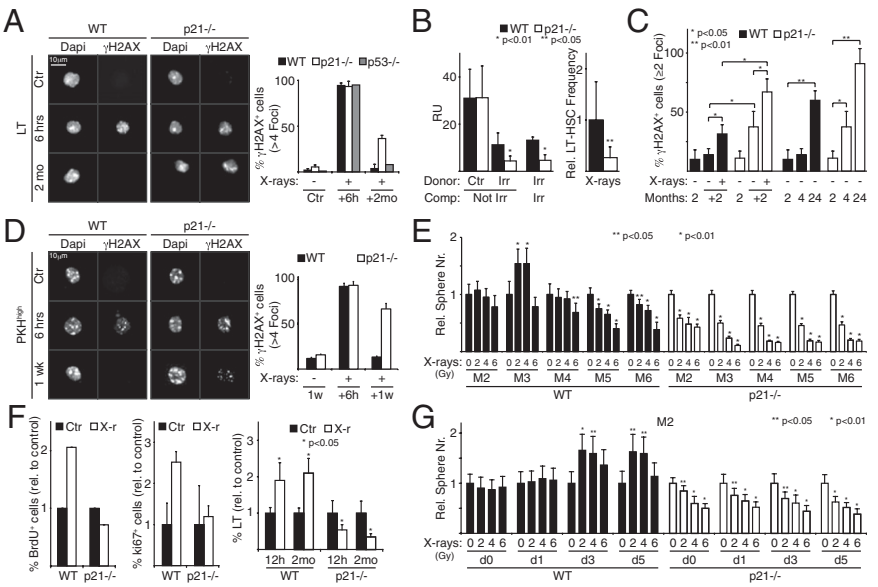

Fig. 4. X-ray–induced p21 up-regulation limits DD accumulation, maintains self-renewal, and promotes expansion of HSCs and MaSCs. (*A*) (*Left*) IF of γH2AX localization in WT, $p21^{-/-}$, and $p53^{-/-}$ Ctr and irradiated LT-HSCs at 6 h and 2 mo after X-ray treatment. (*Right*) Percentage of γH2AX-positive cells (more than four foci per cell). (*B*) (*Left*) Granulocyte chimerism levels (quantified as RU) at 20 wk after competitive transplantation. Donor BM MNCs from Ctr and irradiated (Irr) WT and $p21^{-/-}$ mice were cotransplanted with competitor (Comp) MNCs from nonirradiated (Not Irr) and irradiated (Irr) WT mice. (*Right*) Relative (with respect to WT) frequency of donor LT-HSCs from the same recipients of the same cotransplantation experiment (irradiated donor vs. irradiated competitor). (*C*) Percentage of γH2AX-positive cells (two or more foci per cell) in WT and $p21^{-/-}$ LT-HSCs from 2-mo-old mice (2), irradiated and nonirradiated mice analyzed 2 mo later (+2), and mice during physiological aging (age 2, 4, and 24 mo). (*D*) (*Left*) IF of γH2AX localization in WT and $p21^{-/-}$ Ctr and irradiated PKH^{high} cells at 6 h after irradiation of disaggregated M1 or after one serial passage (1 wk; M2). (*Right*) Percentage of γH2AX-positive cells (more than four foci per cell). (*E*) Relative number (± SD of quadruplicates) of mammospheres formed from irradiated WT and $p21^{-/-}$ M1 after five serial passages (M2–M6), normalized to nonirradiated controls (0 Gy). (*F*) (*Left* and *Center*) Relative frequency of BrdU-positive (Left) and Ki67-positive (Center) WT and $p21^{-/-}$ LT-HSCs at 8 h after irradiation, normalized to nonirradiated controls. (*Right*) Relative frequency of LT-HSCs in the BM of WT and $p21^{-/-}$ mice at 12 h and 2 mo after irradiation, normalized to nonirradiated controls. (*G*) The same experimental analysis as in *E* performed on M2. M1 were disaggregated at day 1, 3, or 5 after plating. Data are expressed as mean ± SD of biological triplicates. *P* values (p) were calculated by Student's *t* test.

at passage M5 and M6) that was further impaired in the irradiated $p21^{-/-}$ mammospheres (from passage M2) (Fig. 4*E*).

These results suggest that p21 regulates the cellular response to DD in both LT-HSCs and MaSCs, limiting DD accumulation and preventing exhaustion of their self-renewal competence. Repair of damaged DNA is not complete, however, leaving SCs with moderate levels of DD and reduced self-renewal.

X-Rays Induce p21-Dependent Cell Cycle Entry and Expansion of HSCs and MaSCs. To investigate how p21 prevents DD accumulation, we analyzed the cell cycle properties of LT-HSCs after X-ray exposure. p21 is involved in the transient cell cycle arrest associated with moderate or low levels of DD in different cell types (20). Mice were subjected to two injections of BrdU given 4-h apart, irradiated concomitantly with the first injection, and killed after 8 or 12 h. Unexpectedly, irradiation increased the percentage of BrdU- and Ki67-positive LT-HSCs measured after 8 h, as well as their absolute numbers measured after 12 h, by approximately twofold (Fig. 4*F*). Of note, this expansion was still detectable at 2 mo after irradiation (Fig. 4*F*). However, irradiation did not increase the frequency of proliferating LT-HSCs in the BM of $p21^{-/-}$ mice and did not affect their absolute number, which actually decreased by ∼50% at both 12 h and 2 mo (Fig. 4*F*). These findings indicate that the X-ray treatment has two effects on LT-HSCs, recruitment into the cell cycle and expansion of absolute numbers, both of which depend on p21.

Analysis of the kinetics of MaSCs during mammosphere formation suggest that they exit the cell cycle after one initial cell division (19). However, we found a 1.5- to 2-fold expansion in M3 number after serial replating of irradiated M1 (Fig. 4*E*), suggesting that X-rays, similar to LT-HSCs, stimulate cell division of MaSCs. This effect was not observed in M2, however (Fig. 4*E*), likely because newly formed MaSCs remain aggregated and then expand into the same sphere when replated to form M2. To test this hypothesis, cell suspensions from M1 were irradiated, disaggregated at different time points (days 1, 3, and 5) and replated to form M2. Under these conditions, the number of M2 at day 3 or 5 was increased by 1.5- to 2-fold, suggesting that MaSCs had undergone a further round of cell division at 2–3 d after irradiation (Fig. 4*G*). As for the LT-HSCs, expansion of MaSCs was p21-dependent (Fig. 4 *E* and *G*).

To investigate the ability of irradiated MaSCs to reconstitute the mammary gland, cell suspensions from WT M1 were irradiated (4 Gy), allowed to form M2, and transplanted under limiting-dilution conditions (from 100,000 to 10 cells) (*SI Appendix*, Fig. S8). Strikingly, the irradiated mammospheres demonstrated increased reconstitution capacity (by ∼2.7-fold; $P < 0.05$) (*SI Appendix*, Fig. S8*C*), confirming that X-rays increase MaSC numbers. Irradiated $p21^{-/-}$ mammospheres were composed mainly of apoptotic cells and were not transplanted.

X-Rays Induce p21-Dependent Symmetric Division of MaSCs by Affecting Levels of p53 Before MaSC Division. Increased proliferation alone does not entirely explain the increase in SCs after X-ray exposure. Under steady-state conditions, SCs undergo asymmetric self-renewing divisions in which one progeny retains the SC identity while the other differentiates, thereby maintaining a fairly constant number of SCs. However, SC numbers can expand, for instance, after tissue injury, owing to symmetric self-renewing divisions, with each SC producing two SCs (19). To examine whether X-rays induce SC symmetric divisions, we analyzed localization of the cell-fate determinant Numb, which in MaSCs is asymmetrically partitioned in the plasma membrane during asymmetric divisions (19). MaSCs were purified from mammospheres as PKH^{high} cells and treated with the cytokinesis inhibitor blebbistatin to allow analysis of Numb distribution immediately after mitosis. Numb formed a clear crescent at the cell membrane of ∼60% nonirradiated PKH^{high} cells ($n = 43$), but was localized uniformly around the cell cortex of ∼70% irradiated PKH^{high} cells ($n = 28$) (Fig. 5*A*), suggesting a switch from asymmetric to symmetric division after X-ray exposure. Analysis of the proliferation potential of the two MaSC daughters, an additional distinguishing feature of symmetric vs. asymmetric divisions (19), yielded similar results (*SI Appendix*, Fig. S9*A*).

We previously showed that unperturbed levels of p53 impose asymmetric MaSC divisions, whereas loss of p53 favors symmetry (19). To investigate the effects of X-rays on p53 activity during the first mitotic division of MaSCs, we monitored the activity of a p53 reporter gene over time. Cell suspensions from M1 were

transduced with a lentivirus expressing a short half-life (<60 min) GFP under a minimal CMV promoter and four copies of a p53-binding site and then plated in methylcellulose. P53 activity was measured at 60-min intervals by quantifying GFP intensity in single MaSCs, identified retrospectively as mammosphere-initiating cells (two representative MaSCs are shown in Fig. 5*B*). For each MaSC, time point data were modeled using linear regression to calculate the slope of the best-fit line up to the mitotic division (m_a). Analysis of nonirradiated MaSCs showed a progressive increase of p53 activity in 19 of 28 divisions, which then decreased sharply in the two daughter cells (m_a = 0.20) (Fig. 5*B* and *SI Appendix*, Fig. S9*B*). No increase in p53 activity level before cell division was observed in 18 of 31 irradiated MaSCs (m_a = 0.06; $P < 0.05$) (Fig. 5 *B* and *C*, and *SI Appendix*, Fig. S9*B*). To correlate the slope of the best-fit lines with division modality (asymmetric vs. symmetric), in the same experiment we classified each MaSC division as asymmetric or symmetric, based on the proliferative behavior of the two daughter cells (19). Strikingly, p53 activity increased markedly before mitosis in 19 of 19 asymmetrically dividing control MaSCs (m_a= 0.28), but did not change or decreased significantly in 18 of 18 symmetrically dividing irradiated MaSCs (m_a= −0.01; $P < 0.01$) (Fig. 5*C* and *SI Appendix*, Fig. S9*C*). These findings demonstrate that asymmetric divisions of MaSCs invariably coincide with increasing levels of p53 activity before the self-renewing mitotic division, and that X-rays prevent p53 accumulation and induce a switch from asymmetric division to symmetric division.

Similar analyses of the $p21^{-/-}$ MaSCs revealed that these cells are resistant to the effects of X-rays. After irradiation, p53 activity levels increased significantly before division, producing an average best-fit line analogous to that of WT control MaSCs (m_a = 0.19) (Fig. 5*C* and *SI Appendix*, Fig. S9*C*), and their modality of division was prevailingly asymmetric (18 of 32 divisions) (Fig. 5*A*). In conclusion, p21 appears to prevent the progressive increase of p53 activity before X-ray–induced mitotic division of MaSCs, thereby influencing the binary fate decision in favor of symmetric division. Of note, in the nonirradiated $p21^{-/-}$ MaSCs, p53 levels did not increase, and the modality of division was skewed toward symmetry (in 25 of 42 divisions), suggesting that other cellular pathways might repress p53 activity in the absence of p21 at steady-state levels.

Discussion

We report here that irradiation of HSCs does not activate p53 or induce apoptosis. The reduced p53 activation in LT-HSCs was surprising, considering that X-rays have been shown to induce p53 in mouse hematopoietic stem progenitor cells (HSPCs) in the absence of apoptosis (12). Of note, however, HSPCs include ∼75% of ST-HSCs (8, 21, 22), suggesting that previous studies on HSPCs might have missed the rare LT-HSCs (∼25%). Indeed, we found activation of p53 in ST-HSCs, which, as reported for HSPCs, were radioresistant. In another study, HSPCs from human cord blood were shown to undergo p53-dependent apoptosis after irradiation (23). The discrepant findings between studies might be related to the different biological properties of BM and cord blood SCs and progenitor cells (2, 3, 24). We noted different effects of X-rays on p53 and apoptosis in LT-HSCs (no p53 activation and no apoptosis), ST-HSCs (p53 activation in the absence of apoptosis), and CMPs/MPPs (p53 activation and apoptosis), suggesting the existence of different DD responses in SC/progenitor populations with distinctive self-renewal and differentiation potentials. Remarkably, we found similar results in MaSCs, suggesting the existence of a unique DD response in adult tissue SCs. Accordingly, a comparable response (attenuated p53 activation and resistance to apoptosis) has been reported for hair follicle bulge SCs (5).

Most significantly, the present study addresses the question of the effects of DD on SC self-renewal. We have shown that DD stimulates SCs to repair damaged DNA and maintain self-renewal, as expected, and also to move into symmetric self-renewal divisions, an unexpected finding (Fig. 6). This results in the expansion of a pool of functional SCs able to support the regeneration of injured tissues. Mechanistically, this response depends on p21 and, at least in part, on its ability to inhibit p53. Irradiation of SCs reduces p53 activity, and this effect might be responsible for the acquisition of symmetric self-renewing abilities, given that basal levels of p53 are known to inhibit symmetric divisions in mammary SCs (19). How p21 is activated in the absence of p53 and how activated p21 favors DNA repair and suppresses p53 remain unclear, however.

Transcription from the p21 promoter can be activated through multiple p53-independent pathways, including the p53 family member p73 and the Checkpoint Kinase 2 (*Chk2*) (25). Indeed, we observed a marked increase in the phosphorylation of *Chk2* in MaSCs after irradiation (*SI Appendix*, Fig. S10), suggesting that Chk2 is involved in the up-regulation of p21 in the absence of p53.

Several lines of evidence support a role for p21 in the activation of DNA repair, based on its ability to bind proliferating cell nuclear antigen , and to regulate, spatially and temporally, several proliferating cell nuclear antigen-interacting proteins

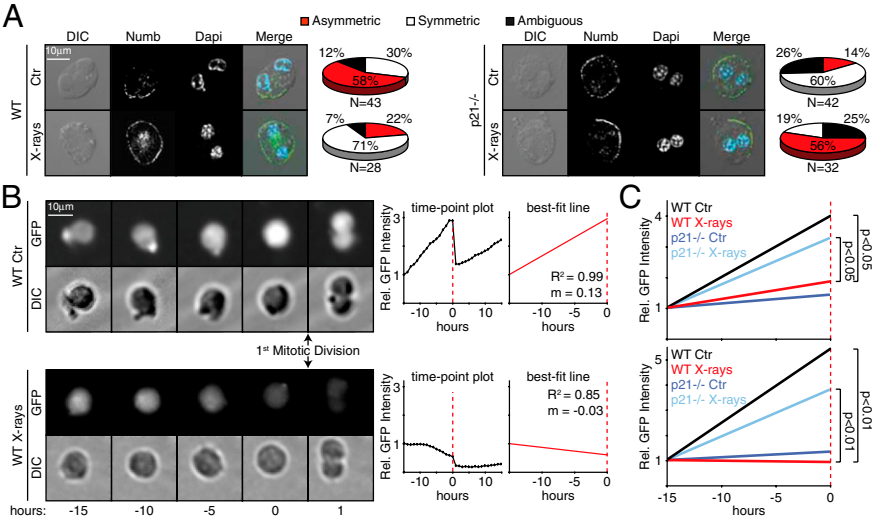

Fig. 5. X-rays induce p21-dependent symmetric division of MaSCs by affecting levels of p53 before division. (*A*) Confocal IF. PKH^{high} cells from WT (*Left*) and $p21^{-/-}$ (*Right*) M1 were treated with blebbistatin for 36 h, irradiated, fixed 6 h later, and stained with anti-Numb and DAPI. DIC, differential interference contrast. The pie charts show relative frequencies of asymmetric and symmetric divisions. (*B*) In vivo fluorescence tracking of p53 activity (GFP intensity) during the first mitotic division of MaSCs. Fluorescence intensity per cell was normalized to its level at 15 h before division. Lines that best approximate the time point data up to the mitotic division (best-fit lines) were obtained by linear regression analysis. Representative images, time point plots, and best-fit lines for one representative control (*Upper*) and one irradiated MaSC (*Lower*) are shown. m, slope of the best-fit line; R^2, coefficient of determination. (*C*) In vivo fluorescence tracking of p53 activity, independent of the modality of division (*Upper Graph*) or linking the slope of best-fit lines with mode of division (asymmetrically-dividing nonirradiated WT or irradiated $p21^{-/-}$ MaSCs compared to symmetrically-dividing irradiated WT or nonirradiated $p21^{-/-}$ MaSCs) (*Lower Graph*). Average best-fit lines (see *SI Appendix*, Fig. S9 *B* and *C*) of control (Ctr) and irradiated WT and $p21^{-/-}$ MaSCs are shown. *P* values were calculated by Student's T test.

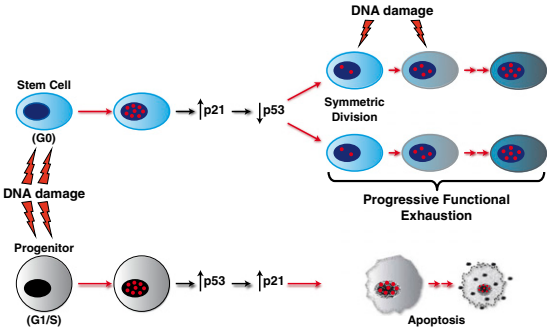

Fig. 6. Effect of X-rays on SCs and progenitors. Irradiation of SCs up-regulates p21, which inhibits p53 basal activity and prevents p53 activation, impeding apoptosis and leading to cell-cycle entry and symmetric self-renewing divisions. p21 also activates DNA repair in SCs, limiting DD accrual and self-renewal exhaustion. DDR is never complete, however, and in response to continuous exposure to DNA-damaging events, SCs progressively accumulate persistent DD and become functionally exhausted. In contrast, progenitor cells respond to X-rays by activating a checkpoint response that involves p53 and its target p21, leading to apoptosis.

involved in different DNA-repair pathways (26). Preliminary results, however, suggest that the SC-associated nonhomologous end joining pathway is not activated in HSCs via p21. Alternatively, p21 may influence the response of SCs to DD by regulating transcription (26). We recently reported that Hes1, a transcriptional-repressor involved in the SC-associated Notch pathway (27), is transcriptionally induced in irradiated SCs in a p21-dependent manner. Depletion of Hes1 renders MaSCs highly susceptible to X-ray–induced apoptosis (*SI Appendix*, Fig. S11), suggesting that Hes1 works as a p21-dependent effector of the DD response in MaSCs. Interestingly, the p53 promoter contains a conserved Hes1 binding site, suggesting that Hes1 might repress transcription of p53 after irradiation.

Regardless of the underlying molecular mechanisms, genetically, the response of SCs to DD is independent of p53. On irradiation, $p53^{-/-}$ SCs up-regulate p21, activate a DNA-repair response, and maintain self-renewal. Thus, p53 is not a key player in the DD response of SCs. How, then, is tumor suppression carried out in SCs? Suppression of apoptosis/senescence, together with high DNA repair activity, might in principle favor accumulation of genomic alterations and transformation of SCs. Repair of damaged DNA in SCs is never complete, however, given that cells with low levels of DD accumulate after irradiation and, crucially, have diminished self-renewal potential (7) (Fig. 4 *A–E* and *SI Appendix*, Fig. S7*D*). Thus, a flawed DDR response in SCs might function physiologically as a mechanism of tumor suppression in these cells. Conversely, overactivation of the same mechanism might contribute to tumor progression. Of note, oncogene expression in HSCs induces DD and activates p21, events critical to maintaining self-renewal in leukemic SCs (28).

Materials and Methods

Mice. All mouse experiments were approved by the Italian Ministry of Health. WT, $p21^{-/-}$, and $p53^{-/-}$ mice were in pure C57BL/6 background.

Image Cytometry. Stained cells were acquired with a robotized fluorescence microscopy station (Scan^R; Olympus) and analyzed using an in-house–developed package based on ImageJ.

Isolation of HSCs, MaSCs, and Progenitor Cells. MNCs were stained with fluorochrome-conjugated antibodies against Sca1, c-Kit, Flk-2, CD34, or the lineage markers (Cd11b, GR1, Ter-119, IL7-R, CD3, CD4, CD8, and B220) and sorted to obtain LT-HSC, ST-HSC, MPP, and CMP subpopulations (28). Mammary cells were stained with PKH-26 dye and sorted to obtain MaSCs and progenitor cells, as described previously (19).

Competitive Transplantation of BM Cells. $Ly5.2^+$ test cells together with WT irradiated or nonirradiated $Ly5.1^+$ cells were injected into lethally irradiated C57BL/6 mice. Variations of SC frequency in the BM were adjusted before transplantation. Donor contribution was assessed in PB samples by FACS analysis of the expression of Ly5.1/ Ly5.2 antigens and quantified by calculating the repopulating units (28).

Intracellular Localization of Numb and Time-Lapse Microscopy. These procedures were performed as described previously (19).

ACKNOWLEDGMENTS. We thank L. Raeli and A. Sciullo for FACS analyses; A. Gobbi, M. Capillo, M. Stendardo, and D. Sardella for help with mice; P. P. Di Fiore for helpful discussions; amd P. Dalton for manuscript editing. This study was supported by grants from the Association for International Cancer Research, the Italian Association for Cancer Research (AIRC), ACLON, the Italian Ministry of Health, the Vollaro Fund, and the De Luise Fund (to P.G.P.).

1. Blanpain C, Mohrin M, Sotiropoulou PA, Passegué E (2011) DNA-damage response in tissue-specific and cancer stem cells. *Cell Stem Cell* 8(1):16–29.
2. Lane AA, Scadden DT (2010) Stem cells and DNA damage: Persist or perish? *Cell* 142(3):360–362.
3. Seita J, Rossi DJ, Weissman IL (2010) Differential DNA damage response in stem and progenitor cells. *Cell Stem Cell* 7(2):145–147.
4. Xu H, et al. (2010) Rad21-cohesin haploinsufficiency impedes DNA repair and enhances gastrointestinal radiosensitivity in mice. *PLoS ONE* 5(8):e12112.
5. Sotiropoulou PA, et al. (2010) Bcl-2 and accelerated DNA repair mediates resistance of hair follicle bulge stem cells to DNA-damage-induced cell death. *Nat Cell Biol* 12(6):572–582.
6. Nijnik A, et al. (2007) DNA repair is limiting for haematopoietic stem cells during ageing. *Nature* 447(7145):686–690.
7. Rübe CE, et al. (2011) Accumulation of DNA damage in hematopoietic stem and progenitor cells during human aging. *PLoS ONE* 6(3):e17487.
8. Rossi DJ, et al. (2007) Deficiencies in DNA damage repair limit the function of haematopoietic stem cells with age. *Nature* 447(7145):725–729.
9. Sedelnikova OA, et al. (2008) Delayed kinetics of DNA double-strand break processing in normal and pathological aging. *Aging Cell* 7(1):89–100.
10. Meek DW (2009) Tumour suppression by p53: A role for the DNA damage response? *Nat Rev Cancer* 9(10):714–723.
11. Levine AJ, Oren M (2009) The first 30 years of p53: Growing ever more complex. *Nat Rev Cancer* 9(10):749–758.
12. Mohrin M, et al. (2010) Hematopoietic stem cell quiescence promotes error-prone DNA repair and mutagenesis. *Cell Stem Cell* 7(2):174–185.
13. Hendry JH, Cai WB, Roberts SA, Potten CS (1997) p53 deficiency sensitizes clonogenic cells to irradiation in the large but not the small intestine. *Radiat Res* 148(3):254–259.
14. Merritt AJ, et al. (1994) The role of p53 in spontaneous and radiation-induced apoptosis in the gastrointestinal tract of normal and p53-deficient mice. *Cancer Res* 54(3):614–617.
15. Qiu W, et al. (2008) PUMA regulates intestinal progenitor cell radiosensitivity and gastrointestinal syndrome. *Cell Stem Cell* 2(6):576–583.
16. Cheng T, et al. (2000) Hematopoietic stem cell quiescence maintained by p21cip1/waf1. *Science* 287(5459):1804–1808.
17. van Os R, et al. (2007) A limited role for p21Cip1/Waf1 in maintaining normal hematopoietic stem cell functioning. *Stem Cells* 25(4):836–843.
18. Rossi DJ, et al. (2007) Hematopoietic stem cell quiescence attenuates DNA damage response and permits DNA damage accumulation during aging. *Cell Cycle* 6(19):2371–2376.
19. Cicalese A, et al. (2009) The tumor suppressor p53 regulates polarity of self-renewing divisions in mammary stem cells. *Cell* 138(6):1083–1095.
20. Ishikawa K, Ishii H, Saito T (2006) DNA damage-dependent cell cycle checkpoints and genomic stability. *DNA Cell Biol* 25(7):406–411.
21. Weissman IL, Shizuru JA (2008) The origins of the identification and isolation of hematopoietic stem cells, and their capability to induce donor-specific transplantation tolerance and treat autoimmune diseases. *Blood* 112(9):3543–3553.
22. Sharpless NE, DePinho RA (2007) How stem cells age and why this makes us grow old. *Nat Rev Mol Cell Biol* 8(9):703–713.
23. Milyavsky M, et al. (2010) A distinctive DNA damage response in human hematopoietic stem cells reveals an apoptosis-independent role for p53 in self-renewal. *Cell Stem Cell* 7(2):186–197.
24. Orkin SH, Zon LI (2008) Hematopoiesis: An evolving paradigm for stem cell biology. *Cell* 132(4):631–644.
25. Aliouat-Denis CM, et al. (2005) p53-independent regulation of $p21^{Waf1/Cip1}$ expression and senescence by Chk2. *Mol Cancer Res* 3(11):627–634.
26. Cazzalini O, Scovassi AI, Savio M, Stivala LA, Prosperi E (2010) Multiple roles of the cell cycle inhibitor p21(CDKN1A) in the DNA damage response. *Mutat Res* 704(1-3):12–20.
27. Davis RL, Turner DL (2001) Vertebrate hairy and Enhancer of split related proteins: Transcriptional repressors regulating cellular differentiation and embryonic patterning. *Oncogene* 20(58):8342–8357.
28. Viale A, et al. (2009) Cell-cycle restriction limits DNA damage and maintains self-renewal of leukaemia stem cells. *Nature* 457(7225):51–56.